Distribution functions of a simple fluid under shear: Low shear rates

Yu. V. Kalyuzhnyi
Institute for Condensed Matter Physics, Svientsitskoho 1, 290011 Lviv, Ukraine

S. T. Cui, P. T. Cummings, and H. D. Cochran
Chemical Technology Division, Oak Ridge National Laboratory, Oak Ridge, Tennessee 37831-6224
and Department of Chemical Engineering, University of Tennessee, Knoxville, Tennessee 37996-2200
(Received 3 February 1999)

Anisotropic pair distribution functions for a simple, soft sphere fluid at moderate and high density under shear have been calculated by nonequilibrium molecular dynamics, by equilibrium molecular dynamics with a nonequilibrium potential, and by a nonequilibrium distribution function theory [H. H. Gan and B. C. Eu, Phys. Rev. A **45**, 3670 (1992)] and some variants. The nonequilibrium distribution function theory consists of a nonequilibrium Ornstein-Zernike relation, a closure relation, and a nonequilibrium potential and is solved in spherical harmonics. The distortion of the fluid structure due to shear is presented as the difference between the nonequilibrium and equilibrium pair distribution functions. From comparison of the results of theory against results of equilibrium molecular dynamics with the nonequilibrium potential at low shear rates, it is concluded that, for a given nonequilibrium potential, the theory is reasonably accurate, especially with the modified hypernetted chain closure. The equilibrium molecular-dynamics results with the nonequilibrium potential are also compared against the results of nonequilibrium molecular dynamics and suggest that the nonequilibrium potential used is not very accurate. In continuing work, a nonequilibrium potential better suited to high shear rates [H. H. Gan and B. C. Eu, Phys. Rev. A **46**, 6344 (1992)] is being tested. [S1063-651X(99)05608-1]

PACS number(s): 05.60.Cd, 05.20.Jj, 05.90.+m

I. INRODUCTION

Kinetic processes are of fundamental interest and importance in many branches of science and engineering, yet theories of nonequilibrium systems have lagged far behind those of equilibrium systems. For example, the theories of equilibrium statistical mechanics provide practical means for calculating the properties of fluids at equilibrium from their structure. And likewise, the structure of fluids at equilibrium, as represented by their pair distribution functions, can be calculated with reasonable accuracy and efficiency using integral equation theories based on the Ornstein-Zernike (OZ) relation with an approximate closure relation, such as the Percus-Yevick (PY) or the hypernetted chain (HNC) equation; see, for example, [1]. The situation is nowhere near so well-developed, however, for systems that are not at equilibrium. Useful theories have been available only for dilute gas systems or for systems only slightly removed from equilibrium, where linear-response theory leads to the linear transport equations with constant transport coefficients, such as Newton's law of viscosity. Evans and Morriss [2] present a well-organized development of the modern statistical mechanics of nonequilibrium fluids and present practical means of determining the properties of nonequilibrium fluids, such as the transport coefficients for viscosity, thermal conductivity, mass diffusivity, etc., from molecular simulation calculations with computers, e.g., calculation of the viscosity of a liquid far from equilibrium by nonequilibrium molecular dynamics (NEMD).

There have been relatively few attempts at theories of dense, nonequilibrium fluids in the nonlinear regime. Approaches based on fluctuating hydrodynamics have been utilized, in which nonrandom fluctuations have been added in a phenomenological way to the macroscopic continuity equations allowing calculation of the density-density correlation function and from it the nonequilibrium radial distribution function and the structure factor; see, for example, [3]. Similarly, Hess [4,5] proposed and solved a phenomenological evolution equation for the nonequilibrium radial distribution function. Gan and Eu (GE) proposed [6,7] an alternative approach and applied it to dense fluids at both low and high shear rates. They derived a heierarchy of nonlinear integral equations for the nonequilibrium fluctuations from the nonequilibrium canonical distribution function, an approach similar in spirit to the theory of the structure of dense equilibrium fluids. The GE theory leads to an integral equation for the anisotropic nonequilibrium pair distribution function which reduces to the PY integral equation in the equilibrium limit, suggesting that the OZ relation also holds for nonequilibrium fluids, i.e., the nonequilibrium OZ equation (NEOZ). In essence, the GE theory postulates a nonequilibrium potential under which the equilibrium structure of a fluid is that of the nonequilibrium fluid.

Unfortunately, the GE theory has not received significant attention or use, and testing to date has been limited. In very recent work [8], Farhat and Eu used the nonequilibrium potential of Gan and Eu [6] in performing Monte Carlo (MC) simulations of a simple fluid under shear; the results showed some deviations from results for the same system by NEMD, reflecting some deficiency or deficiencies in the nonequilibrium potential or the MC algorithm, or in both. Farhat and Gan further showed resasonable agreement between the GE theory and MC, both with the same nonequilibrium potential. Thus, there is considerable promise in the NEOZ approach but no definitive test of its accuracy or reliability. The OZ-based theories of equilibrium fluids have been usefully ex-

tended to complex molecular fluids, even to long-chain polymers [9–11]. If the NEOZ-based theory and the nonequilibrium potential of GE were found to be accurate in definitive testing against simulations, they, too, might be usefully extended for practical applications with complex molecular fluids. If the theory or potential is found to be deficient in such testing, a sound basis is established for seeking improvement.

In this paper, our purpose is to begin exploring the usefulness of the GE theory and to test it against new simulation results generated for this purpose for a simple soft sphere fluid. As an aid to the reader, we summarize the GE theory in Sec. II. In Sec. III we describe our approach to the numerical solution of the NEOZ equation and, in particular, to the versions with the PY closure and with a modified hypernetted chain (MHNC) closure. Special attention is paid to the number of spherical harmonics used in the numerical solution. In Sec. IV we briefly describe our NEMD simulations as well as our equilibrium molecular-dynamics (EMD) calculations with GE's nonequilibrium potential. We present and discuss our results in Sec. V, and we conclude with a few brief remarks in Sec. VI.

II. SUMMARY OF GAN-EU THEORY

To avoid unnecessary repetition, we will present here only a summary of GE theory, focusing mostly on the details which are needed to formulate the final set of equations to be solved. We refer the interested reader to the original publications [6,7]. The point of departure in the OZ theory for the nonequilibrium structure of dense simple fluids is the nonequilibrium distribution function written in the exponential or canonical form suggested by the solution of the generalized Boltzmann equation. This form, with nonequilibrium effects accounted for via the corresponding terms in the potential energy function, is similar to that used in the equilibrium statistical mechanical theory of fluids. The nonequilibrium part of the potential follows from the solution of the set of equations derived from the generalized Boltzmann equation. This set of equations couples the nonequilibrium potential with the macroscopic observables, which are used to describe the nonequilibrium process of interest. Thus, the initial problem of describing the nonequilibrium structure has been substituted by the problem of describing the equilibrium structure with nonequilibrium potential. The latter task is rather straightforward and once the interparticle potential is specified, one can use the whole machinery of the equilibrium statistical mechanical theory of liquids to generate the corresponding OZ equation and its closure conditions. In [6,7] this goal is achieved by formulating the corresponding Kirkwood hierarchy of equations and adopting the Kirkwood superposition approximation together with the assumption that the non-heat-conducting fluid in question undergoes steady shear flow at uniform density and temperature. It is assumed also that the equilibrium interparticle interaction is pairwise additive. As a result, the nonequilibrium analog of the PY equation has been derived. This PY-like equation can be written in the form of the OZ equation, which couples the nonequilibrium direct $c(\boldsymbol{r}_{12},t)$ and total $h(\boldsymbol{r}_{12},t)$ time-dependent pair correlation functions

$$c(\boldsymbol{r}_{12},t)=h(\boldsymbol{r}_{12},t)+\rho\int d\boldsymbol{r}_3 c(\boldsymbol{r}_{13},t)h(\boldsymbol{r}_{32},t) \tag{1}$$

and a PY-like closure relation

$$c(\boldsymbol{r},t)=f_{\mathrm{ne}}(\boldsymbol{r},t)[h(\boldsymbol{r},t)-c(\boldsymbol{r},t)+1], \tag{2}$$

where ρ is the number density, $f_{\mathrm{ne}}(\boldsymbol{r},t)$ is the Mayer function for the nonequilibrium pair potential $V_{\mathrm{ne}}(\boldsymbol{r},t)$, i.e., $f_{\mathrm{ne}}(\boldsymbol{r},t)=\exp[-\beta V_{\mathrm{ne}}(\boldsymbol{r},t)]-1$, and $\beta=1/(k_BT)$.

As one can see, a key quantity of the present theory is the nonequilibrium potential $V_{\mathrm{ne}}(\boldsymbol{r},t)$, which follows from the solution of the corresponding kinetic equation. To proceed further, it is necessary to specify the particular fluid of interest, i.e., its equilibrium potential and shearing flow conditions. Following [6,7], we consider steady-state planar Couette flow of a fluid confined between two infinite parallel plates. The y axis is perpendicular to the plates which are located at $y=\pm\frac{1}{2}D$ and move with a uniform velocity $\pm\frac{1}{2}u_0$ in the opposite directions along the x axis. The corresponding set of equations for the nonequilibrium potential $V_{\mathrm{ne}}(\mathbf{r})$ has been derived and solved in [6,7]. As a result, the following general expression for the nonequilibrium potential has been proposed:

$$V_{\mathrm{ne}}(r,\theta,\phi)=V(r)+\alpha(r)r\frac{\partial V(r)}{\partial r}\left[\frac{\Pi}{2p}\sin^2\theta\sin 2\phi - \frac{1}{3}\frac{N_1}{2p}(2\sin^2\theta\sin^2\phi-1)\right], \tag{3}$$

where $V(r)$ is the equilibrium potential, p is the hydrostatic pressure, Π and N_1 are the shear and normal stresses, respectively, m_r is reduced mass, σ is the size parameter of the particles, γ is the rate of shearing, i.e., $\gamma=(\partial u_x/\partial y)$, u_x is the flow velocity along the x axis, and $\alpha(r)$ is a switching factor

$$\alpha(r)=\begin{cases} g_0(r), & r\leqslant r_0 \\ 1, & r>r_0 \end{cases} \tag{4}$$

which is needed to avoid the infinitely large negative value of $V_{\mathrm{ne}}(\boldsymbol{r})$ for $r=0$. Here, r_0 is defined by the following inequality: $g_0(r)\leqslant 1$ for $0<r\leqslant r_0$ and $g_0(r)$ is the equilibrium pair distribution function of the present system. The shear stress and normal stress satisfy the following algebraic equation:

$$\frac{\overline{\gamma}}{6}\frac{\tau_p p}{\eta_0}\sqrt{\frac{1}{2}\left(1-\frac{4}{9}x^2\right)}+\sinh\left\{\frac{\tau_p p}{\eta_0}\sqrt{\frac{1}{2}\left(\frac{2}{3}x-1\right)}\right\}=0, \tag{5}$$

where

$$\frac{N_1}{2p}=x,\quad \frac{\Pi}{2p}=-\frac{1}{2}\sqrt{-x\left(1+\frac{2}{3}x\right)},$$

$$\overline{\gamma}=\frac{6\eta_0\gamma}{p},\quad \tau_p=\beta\frac{(2\eta_0 m_r^{1/2})^{1/2}}{\rho\sigma(2\beta)^{1/2}},$$

and η_0 is the Newtonian (zero-shear-rate) viscosity. The nonequilibrium potential $V_{ne}(\boldsymbol{r})$ (3) is specialized in the coordinate frame with the azimuthal angle around the z axis denoted as ϕ and the polar angle between vector $\boldsymbol{r}$ and the z axis denoted as θ.

It is assumed that the expression for the nonequilibrium potential (3), which we shall call the full potential, is valid for any degree of departure from equilibrium, i.e., for any values of the shear rate γ. At low values of the shear rate, the contribution from the terms involving the normal stress N_1 can be neglected and for the shear stress Π one can use the Newtonian law of viscosity $\Pi = -\eta_0\gamma$. As a result, for $\overline{\gamma} < 1$ we have

$$V_{ne}(r,\theta,\phi) = V(r) - \frac{\eta_0\gamma}{2p} r \frac{\partial V(r)}{\partial r} \sin 2\phi \sin^2\theta. \tag{6}$$

This expression for the nonequilibrium potential in the low shear limit, proposed in [6,7], will be used for the results presented in this paper; we shall refer to it as the low-shear-rate nonequilibrium potential. Work in progress will examine results with the full potential (3).

As in [6,7], we consider the case of the soft-sphere equilibrium intermolecular potential

$$V(r) = \epsilon\left(\frac{\sigma}{r}\right)^{12}. \tag{7}$$

For this potential, NEMD results for the Newtonian viscosity have been parametrized [12],

$$\eta_0 = [0.171 + 0.022(e^{6.83y} - 1)] \frac{(m\epsilon)^{1/2}}{\sigma^2(\beta\epsilon)^{2/3}}, \tag{8}$$

TABLE I. The shear-rate-dependent viscosity η and pressure for soft-sphere particles at packing fractions $\nu = 0.45$ and $\nu = 0.30$ calculated from NEMD simulations, where the number in the parentheses is the statistical uncertainty in the least significant digits of the corresponding number and t_{run} is the total run length in the reduced time unit τ.

	$\nu = 0.45$			$\nu = 0.3$			
γ^*	η	p^*	t_{run}	γ^*	η	p^*	t_{run}
0.00	1.42(2)	8.389(1)		0.00	0.496(4)	2.666(1)	
0.04	1.423(16)	8.390(1)	2400	0.05	0.498(7)	2.666(1)	2920
0.09	1.404(7)	8.392(1)	3940	0.10	0.496(3)	2.666(1)	5120
0.16	1.409(6)	8.397(1)	1000	0.15	0.496(2)	2.667(1)	4340
0.25	1.389(5)	8.411(1)	1040	0.25	0.492(2)	2.669(1)	3120
0.30	1.391(5)	8.417(2)	660	0.36	0.489(2)	2.673(1)	740
0.36	1.378(4)	8.431(2)	920	0.456	0.487(1)	2.679(1)	2120
0.407	1.372(2)	8.443(1)	4080	0.50	0.484(2)	2.681(1)	940
0.50	1.355(2)	8.468(1)	3200	0.60	0.482(1)	2.689(1)	1180
0.64	1.333(4)	8.514(3)	340	0.689	0.479(1)	2.696(1)	2160
0.75	1.318(1)	8.555(1)	2400	0.80	0.474(1)	2.706(1)	1240
0.814	1.307(2)	8.579(1)	1620	1.00	0.468(1)	2.731(1)	820
1.00	1.277(1)	8.664(1)	980	1.20	0.460(1)	2.757(1)	6540
1.20	1.247(1)	8.678(1)	1320	1.44	0.450(1)	2.794(1)	2780
1.44	1.214(1)	8.904(1)	1660	1.60	0.443(1)	2.831(1)	800
1.60	1.191(1)	9.002(2)	640				

where $y = (1/\sqrt{2})\rho\sigma^3(\beta\epsilon)^{1/4}$ and $m = 2m_r$. This expression for η_0 has been used to calculate the nonequilibrium potential (6).

The expression for the nonequilibrium potential (6) also involves the value of the hydrostatic pressure p, which should be calculated self-consistently for each particular value of the shear rate γ. With this aim one could use the following expression for the pressure tensor $\mathbf{P}$ of the steady-state sheared fluid [13]:

$$\mathbf{P} = \frac{\rho}{\beta}\mathbf{U} - \frac{1}{2}\rho^2 \int d\boldsymbol{r}\, \frac{\boldsymbol{r}\boldsymbol{r}}{r} \frac{\partial V(r)}{\partial r} g(\boldsymbol{r}) \tag{9}$$

which in the present case gives

$$\frac{\beta p}{\rho} = 1 + 4\sqrt{\pi}\rho \int_0^\infty dr\, g_{00}(r) r^{-10}. \tag{10}$$

Here, $\mathbf{U}$ is a unit second-rank tensor and $g_{00}(r)$ is the (00) component of the spherical harmonic expansion of $g(\boldsymbol{r})$. Alternatively, one could use results from NEMD for both the Newtonian viscosity η_0 and the hydrostatic pressure p in calculating the nonequilibrium potential V_{ne}.

Because of the steady-state shearing conditions, the nonequilibrium pair potential (6) as well as the direct and total correlation functions are time-independent. The NEOZ equation and PY closure relation take the following form:

$$\hat{h}(\boldsymbol{k}) = \hat{c}(\boldsymbol{k}) + \rho\hat{c}(\boldsymbol{k})\hat{h}(\boldsymbol{k}) \tag{11}$$

and

$$c(\boldsymbol{r}) = f_{ne}(\boldsymbol{r})[h(\boldsymbol{r}) - c(\boldsymbol{r}) + 1]. \tag{12}$$

The OZ equation (11) is written in terms of the Fourier transforms of the direct and total correlation functions. This form of the OZ equation is more convenient for numerical calculations than the corresponding version of the OZ equation written in the real r space. In addition to the PY closure relation (12), we propose the so-called modified HNC (MHNC) closure with a bridge function $B(\boldsymbol{r})$ chosen in a form proposed by Verlet [14],

$$c(\boldsymbol{r}) = \exp[-\beta V_{ne}(\boldsymbol{r}) + h(\boldsymbol{r}) - c(\boldsymbol{r}) + B(\boldsymbol{r})] - h(\boldsymbol{r}) + c(\boldsymbol{r}) - 1, \tag{13}$$

where

$$B(\boldsymbol{r}) = -\frac{[h(\boldsymbol{r}) - c(\boldsymbol{r})]^2}{2[1 + 0.8h(\boldsymbol{r}) - 0.8c(\boldsymbol{r})]}. \tag{14}$$

For $B(\boldsymbol{r}) = 0$, the present MHNC closure reduces to the HNC type of the closure, proposed in [6,7].

III. NUMERICAL SOLUTION OF THE THEORY

The OZ equation (11) together with its closure relation (12) [or Eq. (13)], relations (10) and (5) form a closed set of

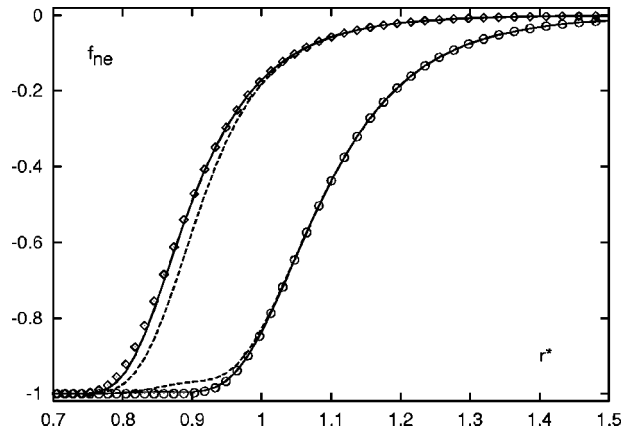

FIG. 1. Mayer function for the low-shear-rate nonequilibrium potential (6) for $\gamma^*=0.75$, $\nu=0.45$, and $p^*=p\epsilon^{-1}\sigma^3=8.56$. Exact results for $\phi=\pi/4$ (circles) and $\phi=3\pi/4$ (diamonds); results with $l_{\max}=4$ (dashed lines) and with $l_{\max}=8$ (solid lines). Here $r^*=r/\sigma$.

equations to be solved. Solution of this set of equations can be obtained by expansion in spherical harmonics as has been utilized in the equilibrium theory of molecular fluids. It consists of expanding the correlation functions in spherical harmonics, writing the initial OZ equation as a set of equations for the spherical harmonic expansion coefficients in Fourier k space, and solving this set using either a direct iteration method or combining the latter with the Newton-Raphson method. This technique is rather standard and details can be found in many places (see, for example, Refs. [15,16]). In the present study, solutions of the corresponding set of equations for the spherical harmonic expansion coefficients have been obtained using the direct iteration method. The forward and inverse Hankel transforms, which are needed to couple the spherical harmonic expansion coefficients in real and Fourier spaces, have been carried out in logarithmic variables, using the method developed by Talman [17]. This

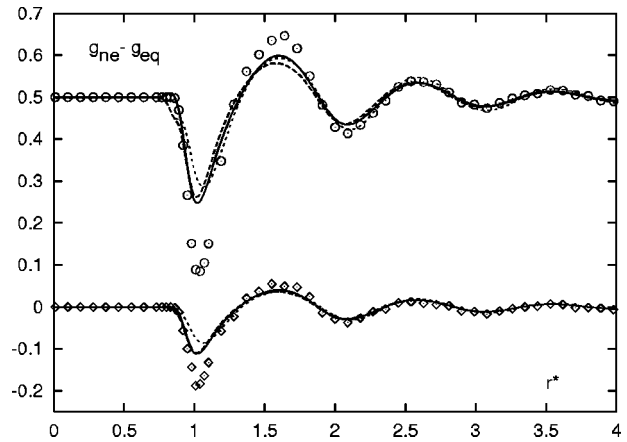

FIG. 2. The distortion of the fluid structure due to shear, $\Delta g_{\rm ne}(r,\theta,\phi)=g_{\rm ne}(r,\theta,\phi)-g_{\rm eq}(r)$, for the system with the low-shear-rate nonequilibrium potential (6) at $\nu=0.45$, $\theta=\pi/2$, $\phi=0$, $\gamma^*=0.75$, and $p^*_{\rm NEMD}=8.56$ (upper portion of the figure) and $\gamma^*=0.5$ and $p^*_{\rm NEMD}=8.47$ (lower portion of the figure). MHNC approximation with $l=8$ (solid lines), MHNC approximation with $l=4$ (long dashed lines), PY approximation with $l=4$ (short dashed line), and EMD (symbols). Here $r^*=r/\sigma$.

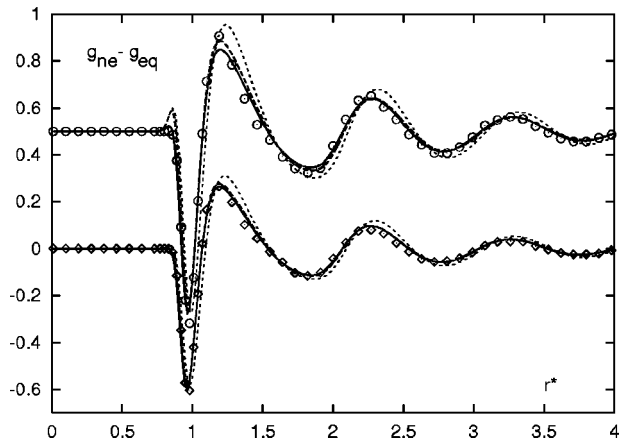

FIG. 3. The same as in Fig. 2 for $\phi=\pi/4$.

method allows us to sample effectively both the rapidly varying part of the correlation functions at small distances and the long-range, slowly decaying portion using a relatively small number of grid points $n=512$, which cover the distance up to $r/\sigma=73$.

IV. MOLECULAR-DYNAMICS SIMULATIONS

Like the theoretical calculations, the molecular-dynamics calculations were performed for a soft-sphere fluid with the equilibrium intermolecular potential (7). For the NEMD calculations, the SLLOD (so named because of its close relationship to the Dolls tensor algorithm) equations of motion [2] were integrated using a velocity Verlet integrator with a Nose thermostat [1]. A time step of 0.002τ was used for the integration, where $\tau=\sigma\sqrt{m/\epsilon}$ is the reduced time unit. The soft-sphere potential was truncated at $r_c=2.0\sigma$, and no long-range correction was applied because it is very small. The EMD calculations with the low-shear-rate potential (6) were carried out in the same way but with the shear rate in the SLLOD equations of motion set to zero. NEMD and EMD calculations were performed with 2048 particles, and relatively long simulations were carried out to ensure that the statistical uncertainties are small.

V. RESULTS AND DISCUSSION

The soft-sphere fluid was studied at two different values of the packing fraction $\nu=\pi/6\rho\sigma^3=0.30$, 0.45 and two dif-

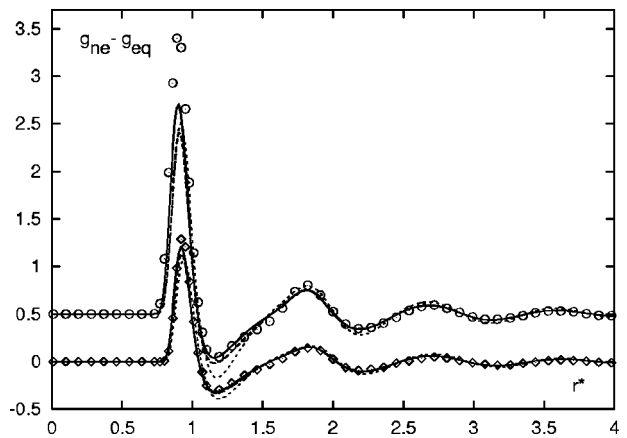

FIG. 4. The same as in Fig. 2 for $\phi=3\pi/4$.

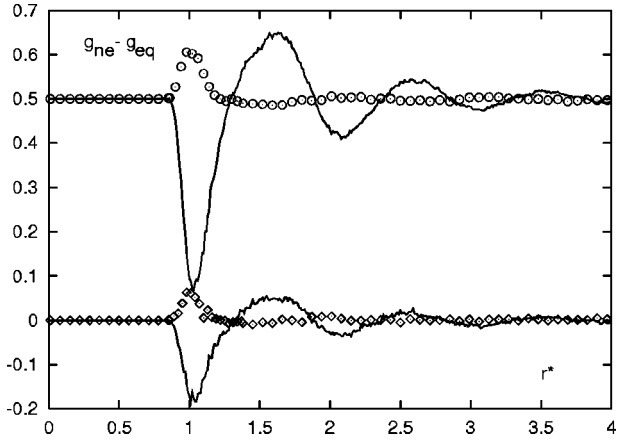

FIG. 5. The distortion of the fluid structure due to shear, $\Delta g_{ne}(r,\theta,\phi)=g_{ne}(r,\theta,\phi)-g_{eq}(r)$ at $\nu=0.45$, $\theta=\pi/2$, $\phi=0$, $\gamma^*=0.75$ (upper portion of the figure), $\gamma^*=0.5$ (lower portion of the figure). EMD with the low-shear-rate nonequilibrium potential (6) (solid lines), NEMD (symbols). Here $r^*=r/\sigma$.

ferent values of reduced shear rate $\gamma^*=\gamma\tau=\gamma\sigma\sqrt{m/\epsilon}$ at each packing fraction. For $\nu=0.45$, we consider the values of the shear rate $\gamma^*=0.50$, 0.75 and for $\nu=0.3$, $\gamma^*=0.456$, 0.689. All the calculations were carried out at reduced temperature value $\beta^*=\beta\epsilon=1$. Table I presents results from the NEMD calculations, including values of the Newtonian viscosity η_0 (obtained by extrapolating the results to zero shear rate) and values of the reduced hydrostatic pressure $p^*=p\epsilon/\sigma^3$ as a function of the reduced shear rate $\gamma^*=\gamma\tau$, which are used as input to some of the theoretical calculations.

As a first step in testing the theory, we compared PY and MHNC results for the pair distribution function $g_{\rm eq}(r)$ of the system with $\nu=0.45$ at equilibrium ($\gamma^*=0$) against corresponding equilibrium molecular-dynamics (EMD) simulation results. As expected, agreement between theoretical results and results of EMD simulation was good, and the agreement was better in the case of MHNC theory. To estimate the number of harmonics $l_{\rm max}$ needed to represent the Mayer function accurately for the nonequilibrium potential (6), in Fig. 1 we compare an exact Mayer function with Mayer functions approximated by a finite number of harmonics. For the shear rate $\gamma^*=0.75$, the Mayer function for the nonequilibrium potential (6) can be accurately represented using eight harmonics. However, with further increase of the shear rate, the number of harmonics needed to describe the Mayer function rapidly increases.

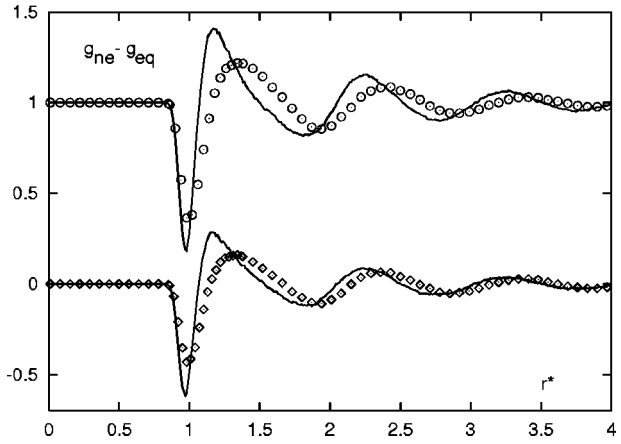

FIG. 6. The same as Fig. 5 but at $\phi=\pi/4$.

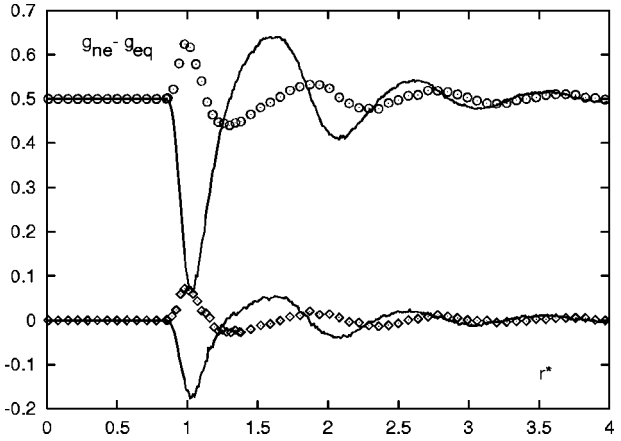

FIG. 7. The same as Fig. 5 but at $\phi=\pi/2$.

In order to test the accuracy of the PY and MHNC theories in reproducing the structure of the system with the low-shear-rate nonequilibrium potential (6), in Figs. 2–4 we illustrate the distortion of the fluid structure due to shear, here defined as $\Delta g_{\rm ne}(r,\theta,\phi)=g_{\rm ne}(r,\theta,\phi)-g_{\rm eq}(r)$, where $g_{\rm ne}$ and $g_{\rm eq}$ are the nonequilibrium and equilibrium pair distribution functions, respectively, for two different values of the shear rate ($\gamma^*=0.5$, 0.75) and at system packing fraction $\nu=0.45$. Here predictions of PY and MHNC theories are compared against the corresponding EMD simulation results for the nonequilibrium potential (6) with hydrostatic pressure obtained from NEMD simulation (Table I). At lower values of the shear rate ($\gamma^*=0.5$), agreement between both theoretical methods and EMD is very good for the values of the azimuthal angle $\phi=\pi/4$ and $\phi=3\pi/4$. For $\phi=0$, PY and MHNC underpredict the depth of the first minimum of the difference $\Delta g_{\rm ne}(r,\theta,\phi)$, with MHNC giving slightly better results. For the higher shear rate ($\gamma^*=0.75$), agreement is also better in the case of MHNC. For $\phi=\pi/4$, agreement is very good; for $\phi=0$, MHNC slightly underpredicts the depth of the first minimum of $\Delta g_{\rm ne}(\boldsymbol{r})$; and for $\phi=3\pi/4$, MHNC

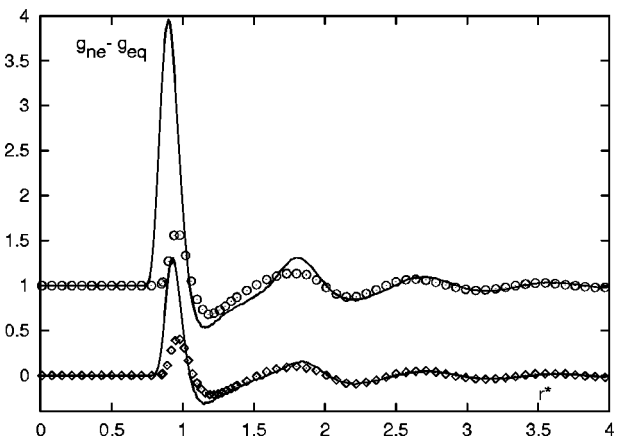

FIG. 8. The same as Fig. 5 but at $\phi=3\pi/4$.

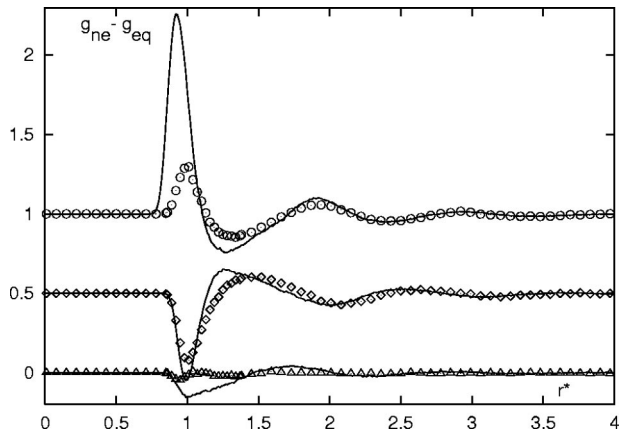

FIG. 9. The distortion of the fluid structure due to shear, $\Delta g_{ne}(r,\theta,\phi)=g_{ne}(r,\theta,\phi)-g_{eq}(r)$, at $\nu=0.3$, $\theta=\pi/2$, $\gamma^*=0.689$, $\phi=0$ (lower portion of the figure), $\phi=\pi/4$ (middle portion of the figure), $\phi=3\pi/4$ (upper portion of the figure). EMD with the low-shear-rate nonequilibrium potential (6) (solid lines), NEMD (symbols). Here $r^*=r/\sigma$.

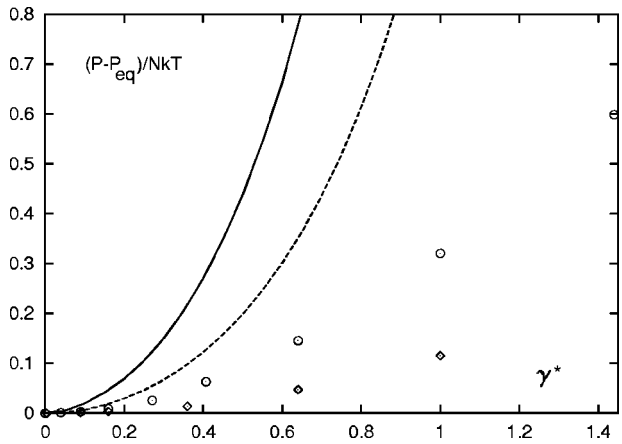

FIG. 10. The difference between the self-consistent value of the pressure and its equilibrium value $(p-p_{eq})/Nk_BT$ as a function of the shear rate γ^* at $\nu=0.45$, NEMD (circles), MHNC approximation for the low-shear-rate nonequilibrium potential (6) (solid line) and at $\nu=0.3$, NEMD (diamonds), MHNC approximation for the low-shear-rate nonequilibrium potential (6) (dashed line).

underpredicts the value of the first maximum. In all cases use of eight harmonics improves the results in comparison with results obtained with only four harmonics.

Next we investigate the accuracy of the low-shear-rate nonequilibrium potential (6) in predicting the nonequilibrium structure of the system in question. This goal can best be achieved by comparing the results from NEMD against results from EMD with the low-shear-rate potential (6). Figures 5–9 make this comparison at two values of the reduced shear rate used by Gan and Eu, $\overline{\gamma}=0.812$ and 0.547 at packing fraction $\nu=0.45$ and at $\overline{\gamma}=0.764$ at packing fraction $\nu=0.3$; the values of $\overline{\gamma}$ have been obtained using values of γ^*, p^* from NEMD (see Table I) and η_0 using the NEMD results parametrization (8). There are notable differences in the magnitude and radial position of peaks in $\Delta g_{ne}(r,\theta,\phi)$ between the NEMD results and the EMD results using the low-shear-rate nonequilibrium potential (6); nevertheless, the low-shear-rate nonequilibrium potential (6) does seem to capture some of the effects of shear on the fluid structure, particularly at the lower shear rate and the lower packing fraction, as would be expected. EMD gives a reasonably accurate prediction for the shift of the first maximum position and for the changes in the phase of oscillation of $g_{ne}(\boldsymbol{r})$ caused be shearing at $\phi=0,\pi/4,\pi/2$. However, the corresponding changes in the magnitude of the first maximum of $g_{ne}(\boldsymbol{r})$ predicted by EMD have an opposite direction in comparison with those predicted by NEMD (see Table II). For the azimuthal angles $\phi=0$ and $\phi=\pi/2$, shearing causes an increase of the first maximum of $g_{ne}(\boldsymbol{r})$, and for $\phi=\pi/4$, a decrease, while EMD predictions are in the opposite directions. Only in the case of $\phi=3\pi/4$ do both EMD and NEMD simulations predict an increase of the first maximum of $g_{ne}(\boldsymbol{r})$ due to shearing. However, at the same time, EMD strongly overestimates this increase. Similar behavior can be seen in the case of the lower packing fraction $\nu=0.3$. One notable artifact of the low-shear-rate nonequilibrium potential (6) is the displacement of the peaks in $g(r)$ to lower values of r at $\phi=3\pi/4$, which results from the $\sin 2\phi$ term, which appears in both the low-shear-rate nonequilibrium potential (6) as well as the full potential (3).

In order to have a complete, self-consistent theory of the nonequilibrium structure of fluids under shear, one might expect to calculate the hydrostatic pressure and the Newton-

TABLE II. Shift in the position Δr_{max} and magnitude $\Delta g_{ne}(r_{max},\theta,\phi)=g_{ne}(r_{max},\theta,\phi)-g_{eq}(r_{max})$ of the first maximum of the nonequilibrium pair distribution function due to shear.

ϕ	Δr_{max}^{EMD}	Δr_{max}^{NEMD}	$\Delta g_{ne}^{EMD}(r_{max},\theta,\phi)$	$\Delta g_{ne}^{NEMD}(r_{max},\theta,\phi)$
0.00	0.01	0.00	−0.405	0.092
$\pi/4$	0.06	0.05	0.124	−0.355
$3\pi/4$	−0.14	−0.04	1.120	0.206

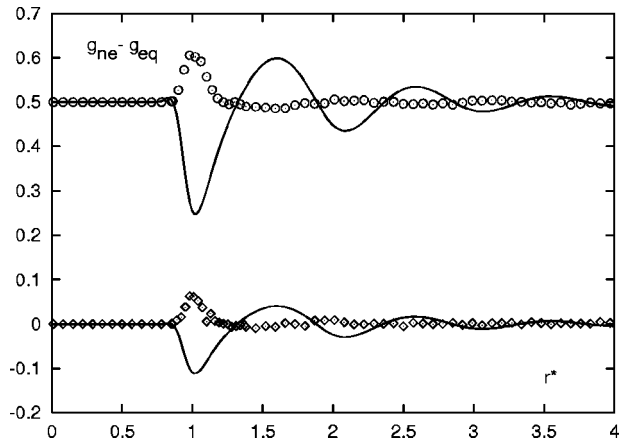

FIG. 11. The distortion of the fluid structure due to shear, $\Delta g_{ne}(r,\theta,\phi)=g_{ne}(r,\theta,\phi)-g_{eq}(r)$, for the system with the low-shear-rate nonequilibrium potential (6) at $\nu=0.45$, $\theta=\pi/2$, $\phi=0$, $\gamma^*=0.75$ (upper portion of the figure), and $\gamma^*=0.5$ (lower portion of the figure). MHNC approximation with the low-shear-rate nonequilibrium potential (6) (solid lines), NEMD (symbols). Here $r^*=r/\sigma$.

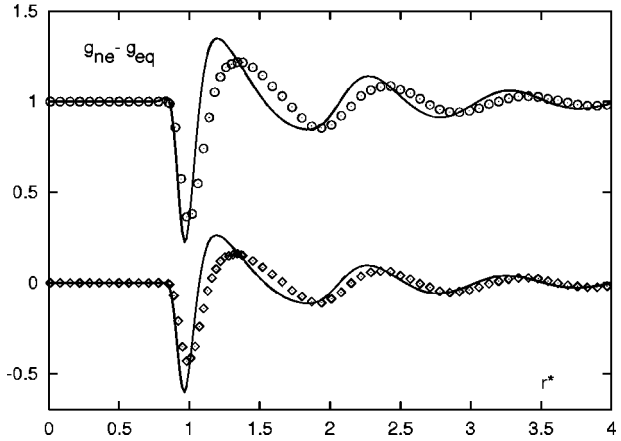

FIG. 12. The same as in Fig. 11 for $\phi=\pi/4$.

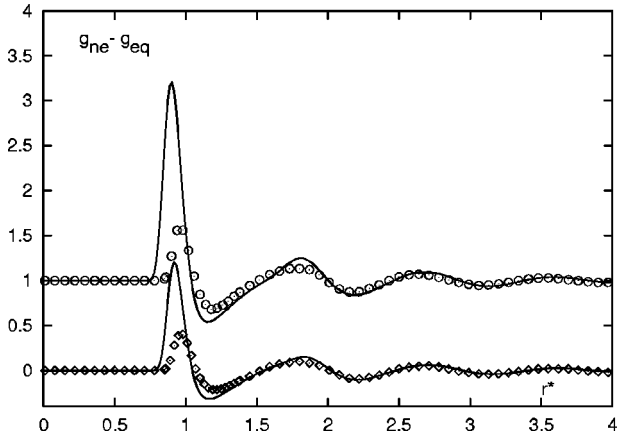

FIG. 14. The same as in Fig. 11 for $\phi=3\pi/4$.

ian viscosity (needed in the nonequilibrium potential) from the theory itself (and not from external simulations or parametrizations thereof). As a first step to this end, we have calculated the hydrostatic pressure self-consistently from the theory using Eq. (10). Figure 10 shows the change of the pressure due to shear $(p-p_{\mathrm{eq}})/Nk_BT$ as a function of shear rate γ^* from the self-consistent MHNC theory with the low-shear-rate nonequilibrium potential (6) and from the NEMD calculations at the two packing fractions $\nu=0.45$ and $\nu=0.30$, respectively. Clearly, the self-consistent MHNC theory with the low-shear-rate nonequilibrium potential predicts the effects of shear on pressure accurately only at very low shear rates.

Now, we have shown that the MHNC theory is quite accurate in predicting the distortion of the structure due to the low-shear-rate nonequilibrium potential (6). We have shown that the low-shear-rate nonequilibrium potential (6) predicts the distortion of the fluid structure by shear only qualitatively. And we have shown that the self-consistent MHNC theory predicts the hydrostatic pressure poorly. We cannot have great hope for the success of the self-consistent MHNC theory with the low-shear-rate nonequilibrium potential (the combining of all the approximate parts of the theory) to predict the distortion due to shear. Nevertheless, for completeness, in Figs. 11–15 we present the distortion of fluid structure due to shear from the theory and from the NEMD calculations. We must conclude that the theory is not very successful.

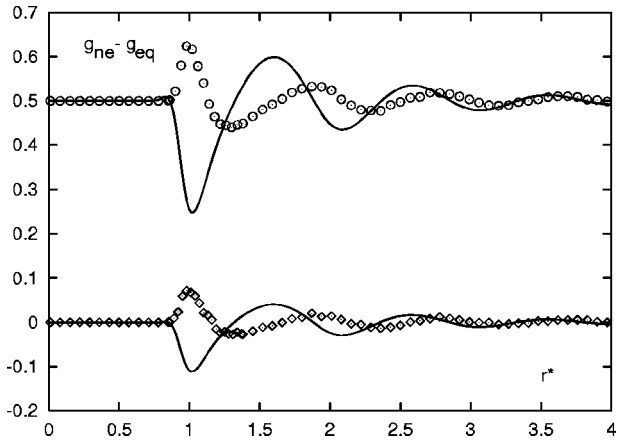

FIG. 13. The same as in Fig. 11 for $\phi=\pi/2$.

VI. CONCLUDING REMARKS

It is an interesting prospect to use the well-developed machinery of equilibrium statistical mechanics with a nonequilibrium potential to predict the structure and properties of fluids in time-invariant, nonequilibrium states such as steady-state shear flow. Gan and Eu's contribution in this regard [6,7] has not been much noticed. Using the methods of NEMD and EMD with a nonequilibrium potential, we have tested the low-shear-rate version of their theory and some variants on it. We find that the OZ relation with a nonequilibrium potential can be used with the PY closure or (better) with the MHNC closure to predict the distortion of the structure of a simple soft-sphere fluid due to the nonequilibrium potential. We find that the low-shear-rate nonequilibrium potential proposed by Gan and Eu [6,7] yields only a qualitative prediction of the distortion of fluid structure due to shear and, when used self-consistently with the theory,

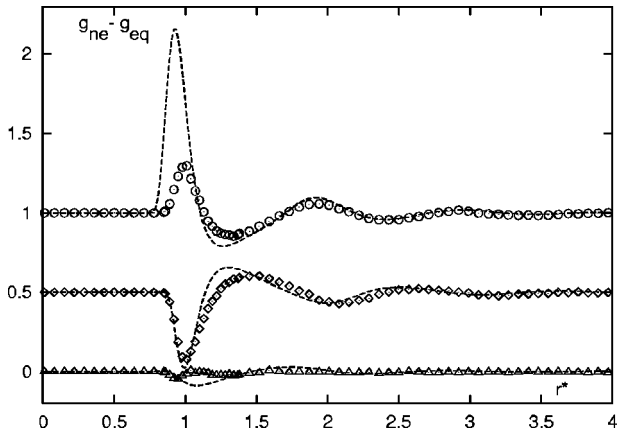

FIG. 15. The distortion of the fluid structure due to shear, $\Delta g_{\mathrm{ne}}(r,\theta,\phi)=g_{\mathrm{ne}}(r,\theta,\phi)-g_{\mathrm{eq}}(r)$, for the system with the low-shear-rate nonequilibrium potential (6) at $\nu=0.3$, $\gamma^*=0.689$, $\theta=\pi/2$, $\phi=0$ (upper portion of the figure), $\phi=\pi/2$ (middle portion of the figure), and $\phi=3\pi/4$ (lower portion of the figure). MHNC approximation for the nonequilibrium potential (6) (solid lines), NEMD (symbols). Here $r^*=r/\sigma$.

yields poor predictions of the effect of shear on hydrostatic pressure except at very low shear rates. Not surprisingly, when the low-shear-rate nonequilibrium potential is used self-consistently, the predictions of combined theory are rather poor. Nevertheless, there still lies hope in the use of an improved nonequilibrium potential. In continuing work [18], we are exploring the performance of the Gan-Eu theory with the full nonequilibrium potential (3), and we are seeking even more accurate models of the nonequilibrium potential.

ACKNOWLEDGMENTS

Y.V.K. is grateful for helpful communications with Professor Eu. This work was supported by the Division of Materials Sciences of the U.S. Department of Energy. Oak Ridge National Laboratory is operated for the U.S. Department of Energy by Lockheed Martin Energy Research Corporation under Contract No. DE-AC05-96OR22464.

[1] J. P. Hansen and I. R. McDonald, *Theory of Simple Liquids*, 2nd ed. (Academic, London, 1986).
[2] D. J. Evans and G. P. Morriss, *Statistical Mechanics of Nonequilibrium Liquids* (Academic, London 1990).
[3] A. M. S. Tremblay, M. Arai, and E. Sigga, Phys. Rev. A **23**, 1451 (1981).
[4] S. Hess, Phys. Rev. A **22**, 2844 (1980).
[5] S. Hess, Physica A **118**, 79 (1983).
[6] H. H. Gan and B. C. Eu, Phys. Rev. A **45**, 3670 (1992).
[7] H. H. Gan and B. C. Eu, Phys. Rev. A **46**, 6344 (1992).
[8] H. Farhat and B. C. Eu, J. Chem. Phys. **110**, 97 (1999).
[9] K. S. Schweizer and J. G. Curro, in *Advances in Polymer Sciences*, edited by L. Monnerie and U. W. Suter (Springer-Verlag, Berlin, 1994), Vol. 116, p. 320.
[10] J. Chang and S. I. Sandler, J. Chem. Phys. **102**, 437 (1995).
[11] Yu. V. Kalyuzhnyi, C.-T. Lin, and G. Stell, J. Chem. Phys. **108**, 6525 (1998).
[12] W. T. Ashurst and W. G. Hoover, Phys. Rev. A **11**, 658 (1975).
[13] J. H. Irwing and J. G. Kirkwood, J. Chem. Phys. **18**, 817 (1950).
[14] L. Verlet, Mol. Phys. **41**, 183 (1980).
[15] C. G. Gray and K. E. Gubbins, *Theory of Molecular Fluids* (Clarendon Press, Oxford, 1984).
[16] S. Labik, R. Pospisil, A. Malijevsky, and W. R. Smith, J. Comput. Phys. **115**, 12 (1994).
[17] J. D. Talman, J. Comput. Phys. **29**, 35 (1978).
[18] S. T. Cui, Yu. V. Kalyuzhnyi, and H. D. Cochran (unpublished).